

A Quantile Nelson-Siegel model *

Matteo Iacopini[†] Aubrey Poon[‡] Luca Rossini[§] Dan Zhu[¶]

July 9, 2025

Abstract

We propose a novel framework for modeling the yield curve from a quantile perspective. Building on the dynamic Nelson–Siegel model of Diebold et al. (2006), we extend its traditional mean-based approach to a quantile regression setting, enabling the estimation of yield curve factors—level, slope, and curvature—at specific quantiles of the conditional distribution. A key advantage of our framework is its ability to characterize the entire conditional distribution of the yield curve across maturities and over time. In an empirical analysis of the U.S. term structure of interest rates, our method demonstrates superior out-of-sample forecasting performance, particularly in capturing the tails of the yield distribution—an aspect increasingly emphasized in the recent literature on distributional forecasting. In addition to its forecasting advantages, our approach reveals rich distributional features beyond the mean. In particular, we find that the dynamic changes in these distributional features differ markedly between the Great Recession and the COVID-19 pandemic period, highlighting a fundamental shift in how interest rate markets respond to distinct economic shocks.

Keywords: Nelson-Siegel; Yield Curve; Bayesian Markov Chain Monte-Carlo; Quantile regression.

*The authors would like to thank Gary Koop and Dimitris Korobilis for their valuable comments on an earlier version of this paper. We also thank seminar and conference participants at the University of Leicester, the Central Bank of Ireland, and the 2025 IAAE Conference for their helpful feedback and suggestions.

[†]Luiss University, Italy. miacopini@luiss.it

[‡]University of Kent, United Kingdom and Örebro University, Sweden. a.poon@kent.ac.uk

[§]University of Milan, Italy and Fondazione Eni Enrico Mattei. luca.rossini@unimi.it

[¶]Monash University, Australia. dan.zhu@monash.edu

1 Introduction

The ongoing global challenges stemming from the COVID-19 pandemic and recent geopolitical conflicts have prompted a renewed focus on inflation and monetary policy. Of particular significance is the information embedded in the term structure of interest rates, offering valuable insights into the evolution of these economic factors. The slope of the yield curve has gained considerable recognition as a key predictor of economic activity, exerting a substantial influence on investors' decision-making processes.

This significance is underscored by research from [Benzoni et al. \(2018\)](#) and [Haubrich \(2021\)](#), which highlights a strong correlation between an inversion of the yield curve and the onset of recessions. For instance, in May 2019, the yield curve inverted almost a year before the commencement of the most recent recession in March 2020. More recently, [Fonseca et al. \(2023\)](#) emphasised the unprecedented inversion in the risk-free yield curves in the United States due to the rapid rise in short-term interest rates since 2022. They pointed out that "*recession probability models based solely on the yield curve slope currently point to elevated odds of recession in the euro area and the United States in one year's time*" thereby stressing the critical importance of dealing with and studying the yield curve in contemporary macroeconomic analysis.

Transitioning to a macroeconomic perspective, significant time variations have been shown to influence the dynamics of US inflation and real activity ([Mumtaz and Surico, 2009](#)). [Mönch \(2012\)](#) studied the evolution of macroeconomic variables by using level, slope, and curvature factors, finding evidence of the informativeness of the curvature factor about the future evolution of the yield curve. Moving to factor analysis, [Coroneo et al. \(2016\)](#) provided evidence that some common factors drive the dynamics of macroeconomic variables and government bonds. More recently, [Fernandes and Vieira \(2019\)](#) predicted the yield curve using different forward-looking macroeconomic variables and highlighted the importance of these variables in forecasting the yield curve.

In the context of modelling the term structure of interest rates, the Nelson-Siegel

(NS) model, introduced by [Nelson and Siegel \(1987\)](#), is the most popular empirical framework employed within the literature. [Diebold and Li \(2006\)](#) generalised this model by introducing smooth dynamics for the latent factors, resulting in the dynamic NS (DNS) model, which outperforms the standard NS approach in an out-of-sample forecasting context. However, these approaches do not account for the potential impact of macroeconomic variables on the yield curve. To address this limitation, [Diebold et al. \(2006\)](#) and [Coroneo et al. \(2016\)](#) analysed the dynamic linkages between yield curve factors and macroeconomic factors in the US. [Koopman and van der Wel \(2013\)](#) found evidence of interdependence between macroeconomic and latent factors in the US term structure, thus supporting the use of macroeconomic variables in combination with financial yield curve factors. Continuing along this line of research, [Bianchi et al. \(2009\)](#) applied a macro-factors augmented DNS model with time-varying parameters to UK data. Recently, [Han et al. \(2021\)](#) introduced a time-varying decay parameter for the arbitrage-free NS model and demonstrated that the relative factor loading reaches its peak just before starting the decline right before a recession.

It is worth emphasising that the literature on the term structure and the analysis of the relationship between yield curve factors and macroeconomic variables so far has been concerned with conditional mean models. However, the in-sample and forecasting performances of this approach are only sufficient in relation to the *mean* of the yields, as the method is not suited to investigate the complete distribution of the yields. To address the limitations of standard conditional mean Nelson-Siegel models and capture the complete picture of the conditional distribution of the yields, we propose a novel quantile regression Nelson-Siegel model with time-varying parameters (TVP-QR-NS) model.

We contribute to this literature by proposing a quantile version of the Nelson-Siegel model for the yield curve. Specifically, we extend the [Diebold et al. \(2006\)](#) 'Yields-Macro' model to a quantile framework. Our approach assumes that the conditional τ -quantile of the yields is given by the Nelson-Siegel three-factor specification, where the

factors are (smoothly) time-varying. Quantile regression (QR, see [Koenker and Bassett, 1978](#)) does not assume a parametric likelihood for the conditional distribution of the response variable. Unlike standard models based on the conditional mean and relying on symmetric second-moment dynamics, our novel framework offers robust modelling of the conditional quantiles, thus enabling a comprehensive investigation of the entire conditional distribution. Moreover, by considering multiple quantile levels, we can follow the method proposed by [Mitchell et al. \(2024\)](#) and combine the quantiles to obtain the distributional yield curve at each point in time, as shown in Figure 1. This permits the investigation of dynamic asymmetry within the distribution of the term structure of interest rates. This feature is particularly crucial when undertaking the modelling and forecasting of interest rate term structures, as emphasised in our empirical application.

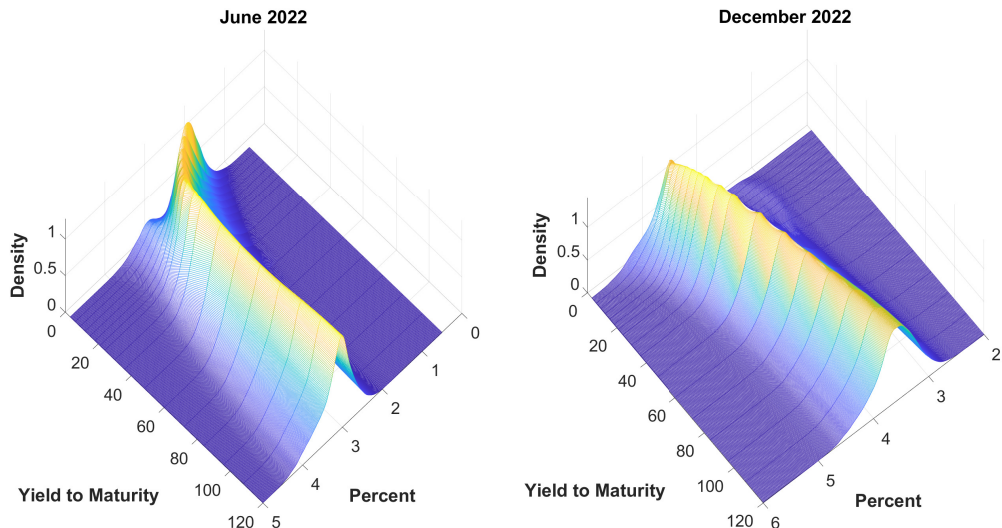


Figure 1: Distributional term structure of the interest rate for June (left) and December (right) 2022.

Inference is performed within a Bayesian framework by leveraging the connection between a likelihood formed by the asymmetric Laplace distribution ([Kotz et al., 2001](#)) and quantile regression provided by [Yu and Moyeed \(2001\)](#), and [Petrella and Raponi \(2019\)](#).

The main feature of the proposed TVP-QR-NS model is the coupling of quantile

regression with time-varying three-factor Nelson-Siegel specification. In addition, to cope with the potentially high dimensionality of the latent dynamic factors, we use a precision sampler (Chan and Jeliazkov, 2009; Chan et al., 2020) that allows us to sample the entire path of the factors jointly without any loop. Overall, this combination provides a simple framework and computationally efficient method to investigate and forecast the term structure at every quantile level of interest. Moreover, our novel econometric framework shares similarities with methodologies put forth by Korobilis and Schröder (2024, 2025). In the former, the authors propose a variational Bayes approach to estimate a quantile static factor model, while the latter extends the factor-augmented vector autoregression to a quantile framework. The primary distinction between our study and both of these lies in our specific focus on analysing the distribution of the yield curve. In contrast, their emphasis is on examining macroeconomic uncertainty within the US and macroeconomic risk across multiple countries.

The proposed method is applied to investigate and forecast the US term structure of interest rates, with particular emphasis on capturing the full distributional dynamics of key yield curve factors. To validate its utility, we conduct an out-of-sample forecasting exercise to evaluate the performance of the TVP-QR-NS model against standard conditional mean benchmarks widely used in the empirical literature. This study contributes to a growing body of research that focuses on forecasting macroeconomic variables from a distributional perspective (see Carriero et al. (2022); Clark et al. (2024); Lenza et al. (2025)). The results indicate that the TVP-QR-NS model consistently delivers superior tail risk forecasts relative to conventional benchmarks, particularly at longer forecast horizons and for long-term maturities. Moreover, employing the model confidence set methodology proposed by Hansen et al. (2011), we find that the TVP-QR-NS model is systematically retained within the confidence sets for longer maturities and long-term forecast horizons, while standard conditional mean models are frequently excluded, underscoring the robustness and reliability of our approach.

The in-sample analysis highlights the advantages of the quantile regression frame-

work over the conventional conditional mean Nelson-Siegel model. Unlike mean-based frameworks, our method enables estimation of the entire distribution of the three Nelson-Siegel factors, as well as yields at selected maturities over time. This comprehensive characterization allows for a more detailed assessment of the effects of recent economic crises, specifically the Great Recession and the COVID-19 pandemic, on the term structure.

The results uncover critical insights that are not accessible through conditional mean models. Specifically, the impact of the Great Recession and COVID-19 on the distribution of short-term interest rates diverges substantially, with clear distributional shifts evident across the two crises. In contrast, the distribution of long-term rates during the Great Recession exhibited no significant shift in location, although an increase in left-skewness was observed.

Further analysis shows that, following the Great Recession, a pronounced location shift occurred across the short, medium, and long ends of the yield curve, with the 10-year maturity exhibiting increased left-skewness. Conversely, during the COVID-19 recession, the location shift was confined to the long end of the yield curve and was accompanied by heightened dispersion. Moreover, we find robust evidence of quantile-dependent dynamics in the relationship between yield curve factors and macroeconomic conditions, underscoring the importance of capturing heterogeneity across the distribution.

The remainder of this article is organised as follows. Section 2 introduces and describes the novel framework, then Section 3 presents the Bayesian approach to inference. Section 4 details the empirical application. Finally, Section 5 concludes.

2 Methodology

2.1 Nelson-Siegel Yield Curve model

The standard Nelson-Siegel (NS) model of the yield curve assumes that

$$y_t(m) = \beta_1 + \beta_2 \left(\frac{1 - \exp^{-\lambda m}}{\lambda m} \right) + \beta_3 \left(\frac{1 - \exp^{-\lambda m}}{\lambda m} - \exp^{-\lambda m} \right), \quad (1)$$

where m denotes the time to maturity; that is, given a set of parameters, *the yield curve* is a deterministic function of maturity. [Diebold and Li \(2006\)](#) pioneered the stochastic modelling of the yield curve and suggested the linear model

$$y_t(m) = \beta_{1t} + \beta_{2t} \left(\frac{1 - \exp^{-\lambda m}}{\lambda m} \right) + \beta_{3t} \left(\frac{1 - \exp^{-\lambda m}}{\lambda m} - \exp^{-\lambda m} \right) + \epsilon_t(m) \quad (2)$$

where $\epsilon_t(m) \sim \mathcal{N}(0, \sigma^2(m))$ is an independent normal innovation. Therefore, given a set of time-varying parameters, the *expected value of the curve* is a deterministic function of maturity.

2.2 A Time-Varying Parameters Quantile NS Model

Assume that $y_t(m) \in \mathcal{Y} \subset \mathbb{R}$ for all maturities $m \in \mathbb{R}_+$, and let $F_t(\cdot; m)$ denote the cumulative distribution function of $y_t(m)$. We propose a new approach that alleviates the parametric assumptions of $y_t(m)$'s by modelling the quantile function of F ,

$$Q_t^\tau(m) = \inf \{x \in \mathcal{Y} : F_t(x; m) \geq \tau\}$$

for each quantile level $\tau \in (0, 1)$ as follows

$$Q_t^\tau(m) = \beta_{1t}(\tau) + \beta_{2t}(\tau) \left(\frac{1 - e^{-\lambda(\tau)m}}{\lambda(\tau)m} \right) + \beta_{3t}(\tau) \left(\frac{1 - e^{-\lambda(\tau)m}}{\lambda(\tau)m} - e^{-\lambda(\tau)m} \right), \quad (3)$$

where m is the maturity, β_{t1}^τ , β_{t2}^τ , and β_{t3}^τ denote the (unobserved) level, slope and curvature factors, and $\lambda(\tau) \in \mathbb{R}_+$ is a decay parameter. Thus, by directly modelling the quantile function, we allow the yield curve factors to behave differently across the quantile levels.

Consider a series of observations at specific maturities $m \in \{1, \dots, M\}$ and denote with $\mathbf{y}_t = (y_t(m_1), \dots, y_t(m_M))'$ the vector of yields at different maturity. Let $\mathbf{x}(m; \lambda(\tau)) = (1, \frac{1-e^{-\lambda(\tau)m}}{\lambda(\tau)m}, \frac{1-e^{-\lambda(\tau)m}}{\lambda(\tau)m} - e^{-\lambda(\tau)m})'$, and $\mathbf{X}(\lambda(\tau)) = [\mathbf{x}(m_1; \lambda(\tau)), \mathbf{x}(m_2; \lambda(\tau)), \dots, \mathbf{x}(m_M; \lambda(\tau))]'$ $\in \mathbb{R}^{M \times 3}$. Then, the conditional quantile model can be written as

$$Q_t^\tau = \mathbf{X}(\lambda(\tau))\boldsymbol{\beta}_t(\tau) \quad (4)$$

such that $Q_t^\tau = (Q_t^\tau(m_1), \dots, Q_t^\tau(m_M))'$ and $\boldsymbol{\beta}_t(\tau) = (\beta_{1t}(\tau), \beta_{2t}(\tau), \beta_{3t}(\tau))'$. Moreover, at each quantile level τ , the unobserved factors are modelled jointly with a vector of macroeconomic (observed) variables $\mathbf{z}_t \in \mathbb{R}^r$. Specifically, the vector of time-varying (unobserved) yield curve and (observed) macroeconomic factors $\boldsymbol{\phi}_t = (\boldsymbol{\beta}_t'(\tau), \mathbf{z}_t')'$ is assumed to follow a stationary VAR(1) process

$$\boldsymbol{\phi}_t = \boldsymbol{\gamma}_0 + \Gamma \boldsymbol{\phi}_{t-1} + \boldsymbol{\eta}_t, \quad \boldsymbol{\eta}_t \sim \mathcal{N}(\mathbf{0}, \Omega). \quad (5)$$

Differently from [Coroneo et al. \(2016\)](#) that proposed an approach related to our in the context of a conditional mean model for the yields, we are modelling the conditional quantile of $y_t(m)$ and rely on an alternative specification of the interactions between the yield and the macroeconomic factors.

To design a regression model for the yield such that the conditional τ -quantile corresponds to eq. (3), we adopt a likelihood-based approach and rely on the properties of the asymmetric Laplace distribution ([Kotz et al., 2001](#)). In particular, for a given quantile τ , we consider a regression model where the innovation follows an asymmetric Laplace distribution $\epsilon_t(m) \sim \mathcal{AL}(\mu, \sigma, \tau)$, with location $\mu \in \mathbb{R}$, scale $\sigma > 0$, skewness

parameter $\tau \in (0, 1)$, with density

$$p(x|\mu, \sigma, \tau) = \frac{\tau(1-\tau)}{\sigma} \exp \left\{ -\rho_\tau \left(\frac{x-\mu}{\sigma} \right) \right\},$$

where $\rho_\tau(x) = x(\tau - \mathbb{I}(x \leq \tau))$ is the check-loss function. Therefore, combining the conditional quantile in eq. (3) with the asymmetric Laplace innovation results in

$$y_t(m) = \mathbf{x}(m; \lambda(\tau))' \boldsymbol{\beta}_t(\tau) + \epsilon_t(m), \quad \epsilon_t(m) \sim \mathcal{AL}(0, \sigma, \tau). \quad (6)$$

It is important to highlight that the asymmetric Laplace distribution admits a stochastic representation as a location-scale mixture of Gaussian (Kotz et al., 2001), thus allowing to rewrite eq. (6) as

$$y_t(m) \stackrel{d}{=} \mathbf{x}(m; \lambda(\tau))' \boldsymbol{\beta}_t(\tau) + w_t(m) \sigma \theta_{\tau,1} + \sqrt{w_t(m)} \sigma \theta_{\tau,2} u_t(m), \quad u_t(m) \sim \mathcal{N}(0, 1), \quad (7)$$

where $w_t(m) \sim \mathcal{Exp}(1)$ is exponential with rate one. To establish an equivalence between the mode of the asymmetric Laplace distribution and the optimisation of the standard quantile regression problem in Koenker and Bassett (1978), the parameters $\theta_{\tau,1}, \theta_{\tau,2}$ are constrained to the following values (Kotz et al., 2001):

$$\theta_{\tau,1} = \frac{1-2\tau}{\tau(1-\tau)}, \quad \theta_{\tau,2} = \sqrt{\frac{2}{\tau(1-\tau)}}. \quad (8)$$

In the existing literature, the decay parameter is often fixed at $\lambda = 0.0609$ (e.g., Diebold and Li, 2006). In contrast, we adopt an agnostic approach by estimating $\lambda(\tau)$ separately for each quantile, and assume a uniform prior distribution, $\lambda(\tau) \sim \mathcal{U}(0, 0.3)$ (see the appendix for further details). Given that the conditional posterior distribution of $\lambda(\tau)$ is non-standard, we employ a Griddy-Gibbs sampling step to draw from its posterior. Finally, the scale of the innovation is set to $\sigma = 1.0$, as in the original quantile regression model (Yu and Moyeed, 2001).

The combination of eq. (5) and (6) provides the state-space form of the proposed time-varying parameters quantile Nelson-Siegel model (TVP-QR-NS) as

$$\begin{aligned} y_t(m) &= \mathbf{x}(m; \lambda(\tau))' \boldsymbol{\beta}_t(\tau) + \epsilon_t(m), \quad \epsilon_t(m) \sim \mathcal{AL}(0, \sigma, \tau) \\ \boldsymbol{\phi}_t &= \boldsymbol{\gamma}_0 + \Gamma \boldsymbol{\phi}_{t-1} + \boldsymbol{\eta}_t, \quad \boldsymbol{\eta}_t \sim \mathcal{N}(\mathbf{0}, \Omega), \end{aligned} \tag{9}$$

Denoting with $\mathbf{Y} = (\mathbf{y}_1, \dots, \mathbf{y}_T)' \in \mathbb{R}^{T \times M}$ the matrix of observations, the joint density of the observables and auxiliary variables (conditional on the time-varying factors) is

$$p(\mathbf{Y}, \mathbf{w} | \boldsymbol{\beta}) = \prod_{m=1}^M \mathcal{E}xp(w_t(m)|1) \times \mathcal{N}(y_t(m) | \mathbf{x}(m; \lambda(\tau))' \boldsymbol{\beta}_t(\tau) + w_t(m) \sigma \theta_{\tau,1}, w_t(m) \sigma^2 \theta_{\tau,2}^2). \tag{10}$$

3 Estimation

This section is devoted to the prior description and the derivation of the precision sampler algorithm.

3.1 Prior Specification

We consider a multivariate Gaussian prior for the initial value of the time-varying factors:

$$\boldsymbol{\beta}_0(\tau) \sim \mathcal{N}(\underline{\boldsymbol{\mu}}_{\beta}, \Sigma_{\beta}). \tag{11}$$

By leveraging the mixture representation of the asymmetric Laplace distribution, we obtain a conditionally linear Gaussian state space for the latent dynamic vector $\boldsymbol{\beta}_t$. Thus, we sample the full conditional posterior distribution of $\boldsymbol{\beta}_t$ directly in a single loop, using a precision sampler (e.g., see [Chan and Jeliazkov, 2009](#); [Chan et al., 2020](#)) as described in the following subsection.

Let us define $e_t(m) = y_t(m) - \mathbf{x}(m; \lambda(\tau))' \boldsymbol{\beta}_t$. Then, the full conditional posterior

distribution of the auxiliary variable $w_t(m)$ is obtained as

$$w_t(m)|y_t(m), \boldsymbol{\beta}_t \propto w_t(m)^{-\frac{1}{2}} \exp \left\{ -\frac{1}{2} \left[\frac{\theta_{\tau,1}^2}{\theta_{\tau,2}^2} w_t(m) + 2w_t(m) + w_t(m)^{-1} \frac{e_t(m)^2}{\theta_{\tau,2}^2 \sigma^2} \right] \right\}, \quad (12)$$

which is the kernel of the generalized inverse Gaussian distribution $\text{GiG}(\bar{p}_w, \bar{a}_w, \bar{b}_{w,m,t})$ with

$$\bar{p}_w = 1 - \frac{1}{2}, \quad \bar{a}_w = 2 + \frac{\theta_{\tau,1}^2}{\theta_{\tau,2}^2}, \quad \bar{b}_{w,m,t} = \frac{e_t(m)^2}{\theta_{\tau,2}^2 \sigma^2}.$$

Finally, we specify a Gaussian prior for the vectorised coefficient matrix of the state equation, $\boldsymbol{\gamma} = (\boldsymbol{\gamma}'_0, \text{vec}(\Gamma)')'$, and an inverse Wishart prior for the innovation covariance, that is

$$\boldsymbol{\gamma} \sim \mathcal{N}(\underline{\boldsymbol{\mu}}_\Gamma, \underline{\Sigma}_\Gamma), \quad \Omega \sim \mathcal{IW}(\underline{v}, \underline{V}). \quad (13)$$

As the prior distributions are conjugate, the full conditional posteriors are straightforward to obtain as

$$\boldsymbol{\gamma}|\boldsymbol{\phi}, \Omega \sim \mathcal{N}(\bar{\boldsymbol{\mu}}_\Gamma, \bar{\Sigma}_\Gamma), \quad \Omega|\boldsymbol{\phi}, \gamma_0, \Gamma \sim \mathcal{IW}(\bar{v}, \bar{V}). \quad (14)$$

The derivation of these full conditional posteriors is standard (e.g, see [Chan, 2020](#)).

3.2 The precision sampler

While the conditional distribution of the parameters given the data and the set of unobserved latent factors is relatively standard, the most significant computational costs arise from sampling the large number of latent factors, denoted as $\boldsymbol{\beta}_t(\tau)$.

Let us start by rewriting the measurement equation in (9) in compact form by stacking all observations together. Specifically, we define the stacked vectors $\mathbf{y} = (\mathbf{y}'_1, \dots, \mathbf{y}'_T)', \boldsymbol{\beta} = (\boldsymbol{\beta}_1(\tau)', \dots, \boldsymbol{\beta}_T(\tau)')', \mathbf{w} = (w_1, \dots, w_T)',$ and $\mathbf{u} = (u_1, \dots, u_T)',$ we

have

$$\mathbf{y} = (\mathbf{I}_T \otimes \mathbf{X}(\lambda(\tau))) \boldsymbol{\beta} + \theta_{\tau,1} \sigma \mathbf{w} + \mathbf{u}, \quad (15)$$

where $\mathbf{u} \sim \mathcal{N}(\mathbf{0}_{TM}, \sigma^2 \theta_{\tau,2} \Omega_1)$ with $\Omega_1 = \text{diag}(\mathbf{w})$. Similarly, we define $\boldsymbol{\phi} = (\boldsymbol{\phi}'_1, \dots, \boldsymbol{\phi}'_T)'$ and rewrite the state equation in a matrix form as

$$\mathbf{H}\boldsymbol{\phi} = \tilde{\boldsymbol{\gamma}} + \boldsymbol{\eta}, \quad \boldsymbol{\eta} \sim \mathcal{N}(\mathbf{0}_{T(r+3)}, \Omega \otimes \mathbf{I}_T), \quad (16)$$

where

$$\mathbf{H} = \begin{pmatrix} \mathbf{I}_{r+3} & \mathbf{0}_{r+3} & \mathbf{0}_{r+3} & \mathbf{0}_{r+3} & \dots & \mathbf{0}_{r+3} & \mathbf{0}_{r+3} \\ \mathbf{0}_{r+3} & -\Gamma & \mathbf{I}_{r+3} & \mathbf{0}_{r+3} & \dots & \mathbf{0}_{r+3} & \mathbf{0}_{r+3} \\ \dots & \dots & \dots & \dots & \dots & \dots & \dots \\ \dots & \dots & \dots & \dots & \dots & \mathbf{I}_{r+3} & \mathbf{0}_{r+3} \\ \dots & \dots & \dots & \dots & \dots & -\Gamma & \mathbf{I}_{r+3} \end{pmatrix}, \quad \tilde{\boldsymbol{\gamma}} = \begin{pmatrix} \boldsymbol{\gamma}_0 \\ \boldsymbol{\gamma}_0 \\ \dots \\ \boldsymbol{\gamma}_0 \\ \boldsymbol{\gamma}_0 \end{pmatrix}.$$

Note that the unobserved factors are placed first in the VAR vector such that

$$\boldsymbol{\phi} = S_1 \boldsymbol{\beta} + S_2 \mathbf{u},$$

where

$$S_1 = \mathbf{I}_T \otimes (\mathbf{I}_3, \mathbf{0}_{3 \times r})', \quad S_2 = \mathbf{I}_T \otimes (\mathbf{0}_{3 \times r}, \mathbf{I}_r)'.$$

Thus, we obtain the conditional posterior of the time-varying yield curve factors as $\boldsymbol{\beta} | \mathbf{Y}, \mathbf{w}, \Gamma, \boldsymbol{\gamma}_0, \Omega \propto \mathcal{N}(\boldsymbol{\mu}_b, K_b^{-1})$, where

$$K_b = \frac{1}{\sigma^2 \theta_{\tau,2}} (\mathbf{I}_T \otimes \mathbf{X}(\lambda(\tau)))' \Omega_1^{-1} (\mathbf{I}_T \otimes \mathbf{X}(\lambda)) + S_1 \mathbf{H}' (\mathbf{I}_T \otimes \Omega^{-1}) \mathbf{H} S_1,$$

$$\boldsymbol{\mu}_b = K_b^{-1} \left((\mathbf{I}_T \otimes \mathbf{X}(\lambda(\tau)))' \Omega_1^{-1} (\mathbf{y} - \theta_{\tau,1} \sigma \mathbf{w}) + S_1 \mathbf{H}' (\mathbf{I}_T \otimes \Omega^{-1}) (\boldsymbol{\gamma} - \mathbf{H} S_2 z) \right).$$

3.3 Monotonicity

Traditional estimation of quantile regression, including our strategy, involves fitting the quantile NS model separately at each quantile level, treating each quantile as an independent modeling task. Although this approach provides flexibility and ease of implementation, it overlooks the intrinsic monotonicity that should characterize conditional quantile functions by construction. As a result, the estimated quantile curves may violate the logical ordering across quantiles, potentially leading to internal inconsistencies and undermining the interpretability of the distributional forecasts.

To ensure monotonicity across quantile levels $\tau \in \{\tau_1, \dots, \tau_K\}$, it is essential to move beyond separate estimations and instead estimate the quantile NS models jointly across τ . This joint estimation framework requires imposing explicit monotonicity constraints across quantiles,

$$\mathbf{x}(m; \lambda(\tau_k))' \boldsymbol{\beta}_t(\tau_k) \leq \mathbf{x}(m; \lambda(\tau_{k+1}))' \boldsymbol{\beta}_t(\tau_{k+1})$$

for $m = 1, \dots, M, k = 1, \dots, K$ and $t = 1, \dots, T$, thus preserving the fundamental ordering structure inherent to conditional quantile functions. However, this approach introduces a large number of cross-quantile constraints, and the resulting optimization problem becomes highly complex and computationally burdensome, to the point where joint estimation under monotonicity constraints can be practically infeasible in its full form. This poses a major challenge for implementing a theoretically coherent yet computationally tractable distributional forecasting framework. To construct a coherent predictive density from the individually estimated quantile NS models, we adopt the re-ordering technique proposed by Chernozhukov et al. (2010), a standard approach in the literature for addressing the issue of quantile crossing.

In the context of the NS model, the yield curve is endowed with additional structural interpretation that can inform both estimation and inference. Specifically, the level factor in the NS model captures the long-run component of interest rates and asymptotically corresponds to the yield at extremely long maturities—essentially representing

the ultimate long-term rate. Conversely, the sum of the level and slope factors determines the instantaneous (short-term) interest rate, reflecting the yield at the shortest maturity. Based on these insights, we can potentially impose the following monotonicity constraints

$$\beta_{t,1}(\tau_k) \leq \beta_{t,1}(\tau_{k+1}) \quad (17)$$

and

$$\beta_{t,1}(\tau_k) + \beta_{t,2}(\tau_k) \leq \beta_{t,1}(\tau_{k+1}) + \beta_{t,2}(\tau_{k+1}). \quad (18)$$

Instead of directly imposing these monotonicity constraints within a joint estimation framework—such as through constrained MCMC, which would be computationally intensive—we adopt a more practical post-processing strategy. Specifically, we formulate a quadratic programming problem that adjusts the unconstrained estimates of $\beta_{t,1}(\tau_k)$ and $\beta_{t,2}(\tau_k)$ across quantile levels. The objective is to find new values that remain as close as possible to the originally estimated posterior mean, $\hat{\beta}_{t,1}$ and $\hat{\beta}_{t,2}$, while satisfying the monotonicity constraints. This post-estimation correction ensures internal consistency and preserves the structural interpretation of the NS model, while avoiding the computational burden of imposing constraints during the sampling phase.

4 Empirical Application

This section focuses on evaluating the performance of the proposed TVP-QR-NS model applied to zero-coupon US Treasury yields. Specifically, the analysis is divided into two parts: an out-of-sample forecasting exercise and an in-sample assessment.

4.1 Data

Our empirical investigation employs zero-coupon US Treasury yields as constructed by [Liu and Wu \(2021\)](#) through a non-parametric kernel smoothing methodology. The application of this novel yield curve dataset by [Liu and Wu \(2021\)](#) is demonstrated to

offer a more precise depiction of the underlying data when compared to the alternative metric presented by [Gürkaynak et al. \(2007\)](#). Following the methodology established by [Diebold et al. \(2006\)](#), our analysis encompasses zero-coupon US Treasury maturities spanning 3, 6, 9, 12, 15, 18, 21, 24, 30, 36, 48, 60, 72, 84, 96, 108, and 120 months. Additionally, our investigation includes key monthly macroeconomic indicators — Industrial Production, CPI Inflation, and the Fed Funds Rate — in line with the framework suggested by [Diebold et al. \(2006\)](#). These macroeconomic variables are chosen to capture the dynamic aspects of the macroeconomy and are all sourced from the US FRED database. Both Industrial Production and CPI Inflation were transformed to log-differenced growth rates. Our study period extends from November 1971 to December 2024.

4.2 Forecasting Yields Tail Risk

To validate the utility of our proposed framework, we conduct a pseudo-out-of-sample forecasting exercise to evaluate the performance of the quantile Nelson-Siegel approach in capturing tail risks in zero-coupon yields. The benchmark model employed for comparison is a univariate autoregressive model with one lag. Our proposed model's performance is assessed relative to this baseline as well as three alternative conditional mean models, as detailed in Table 1. These competing specifications include: (i) a time-varying parameter model with stochastic volatility (SV); (ii) the large Bayesian vector autoregression (VAR) with common stochastic volatility (CSV) developed by [Chan \(2020\)](#); and (iii) the conditional mean formulation of the dynamic Nelson-Siegel model of [Diebold et al. \(2006\)](#).

Table 1: Overview of Competing Models

Model	Description
AR(1)	Autoregressive model with one lag (Benchmark model).
TVP-AR(1)-SV	Time-varying parameter autoregressive model with SV and one lag.
BVAR(1)-CSV	Large Bayesian VAR with one lag and common stochastic volatility.
DNS	Dynamic Nelson-Siegel model of Diebold et al. (2006) .
TVP-QNS	Proposed Quantile-based time-varying Nelson-Siegel model.

The initial holdout period spans from November 1971 to January 2000, with a subsequent forecast evaluation period extending from February 2000 to December 2024. We generate 1st, 12th, and 36th month-ahead tail risk forecasts and evaluate the predictive performance of the competing models using the quantile score (QS) (see [Giacomini and Komunjer, 2005](#); [Carriero et al., 2022](#)). Following [Gneiting and Ranjan \(2011\)](#), we define the QS as:

$$QS_{\tau,i,t} = (y_t(m) - \mathcal{Q}_{\tau,i,t}) - (\tau - \mathbb{I}\{y_t(m) \leq \mathcal{Q}_{\tau,i,t}\}). \quad (19)$$

Here, $\mathcal{Q}_{\tau,i,t}$ denotes the predictive quantile of the m -th yield, and $\mathbb{I}\{y_t(m) \leq \mathcal{Q}_{\tau,i,t}\}$ takes the value 1 if the realised value is at or below the predictive quantile and 0 otherwise. We evaluate the QS in the upper and lower tails by setting $\tau = 0.9$ and $\tau = 0.1$, respectively.

Table 2: Average 10% (Lower-Tail) Quantile Scores for Selected Maturities Relative to an AR(1) Benchmark

Model	3m	p_{MCS}	6m	p_{MCS}	12m	p_{MCS}	24m	p_{MCS}	36m	p_{MCS}	60m	p_{MCS}	120m	p_{MCS}	Avg.
<i>1 Month-Ahead Forecast</i>															
TVP-AR(1)-SV	0.43	0.00	0.42	0.01	0.50	0.03	0.63	0.02	0.72	0.00	0.81	0.00	0.90	0.00	0.68
BVAR(1)-CSV	0.28	1.00**	0.31	1.00**	0.38	1.00**	0.50	1.00**	0.57	0.64**	0.63	0.23*	0.65	1.00**	0.52
DNS	1.72	0.00	1.32	0.00	1.06	0.00	1.13	0.00	1.23	0.00	1.29	0.00	1.07	0.00	1.20
TVP-QNS	0.48	0.00	0.46	0.00	0.47	0.04	0.53	0.46**	0.55	1.00**	0.57	1.00**	0.70	0.41**	0.55
<i>12 Month-Ahead Forecast</i>															
TVP-AR(1)-SV	1.60	0.00	1.27	0.00	1.39	0.00	1.27	0.00	1.07	0.00	0.94	0.00	0.88	0.00	1.15
BVAR(1)-CSV	0.73	0.18*	0.77	0.18*	0.82	0.17*	0.90	0.18*	0.93	0.18*	0.94	0.18*	0.91	0.18*	0.88
DNS	1.15	0.00	1.10	0.00	1.05	0.00	1.08	0.00	1.11	0.00	1.13	0.00	1.04	0.00	1.09
TVP-QNS	0.76	1.00**	0.75	1.00**	0.73	1.00**	0.76	1.00**	0.76	1.00**	0.74	1.00**	0.64	1.00**	0.73
<i>36 Month-Ahead Forecast</i>															
TVP-AR(1)-SV	—	0.00	—	0.00	—	0.00	—	0.00	—	0.00	—	0.00	2.84	0.00	—
BVAR(1)-CSV	1.13	0.00	1.17	0.00	1.19	0.00	1.24	0.00	1.26	0.00	1.27	0.00	1.25	0.00	1.23
DNS	1.04	0.00	1.03	0.00	1.01	0.00	1.05	0.00	1.08	0.00	1.12	0.00	1.10	0.00	1.07
TVP-QNS	0.79	1.00**	0.79	1.00**	0.79	1.00**	0.84	1.00**	0.86	1.00**	0.87	1.00**	0.79	1.00**	0.83

Notes: Superscripts * and ** indicate inclusion in the model confidence sets $\widehat{\mathcal{M}}_{90\%}^*$ and $\widehat{\mathcal{M}}_{75\%}^*$ respectively, as per [Hansen et al. \(2011\)](#). The reported average score is computed across all 17 maturities. A dash (‘-’) indicates that the quantile scores for the TVP-AR(1)-SV model are exceptionally large and thus omitted from the table for clarity.

Tables 2 and 3 present the 10th and 90th percentile quantile scores (QS) from the out-of-sample forecasting exercise for selected maturities. We also report the corresponding p-values from the Model Confidence Set (MCS) procedure proposed by [Hansen et al. \(2011\)](#). The results suggest that the proposed quantile Nelson-Siegel model delivers superior tail risk forecasts, particularly at longer forecast horizons and for long-term maturities. At shorter horizons, however, the BVAR(1)-CSV model remains competitive and, in some cases, outperforms the proposed model in forecasting tail risks. Importantly, the quantile Nelson-Siegel model consistently outperforms its conditional mean counterparts, based on [Diebold et al. \(2006\)](#), across all forecast horizons and quantile levels. Moreover, the MCS analysis shows that the proposed model is always included

in the $\widehat{\mathcal{M}}_{90\%}^*$ and $\widehat{\mathcal{M}}_{75\%}^*$ confidence sets, especially for longer maturities and extended forecast horizons. By contrast, the three conditional mean models are frequently excluded from these sets. Overall, these findings provide strong empirical support for the proposed time-varying parameter quantile Nelson-Siegel model as a robust tool for forecasting tail risk.

Table 3: Average 90% (Upper-Tail) Quantile Scores for Selected Maturities Relative to an AR(1) Benchmark

Model	3m	p_{MCS}	6m	p_{MCS}	12m	p_{MCS}	24m	p_{MCS}	36m	p_{MCS}	60m	p_{MCS}	120m	p_{MCS}	Avg.
<i>1 Month-Ahead Forecast</i>															
TVP-AR(1)-SV	0.37	0.00	0.39	0.01	0.49	0.03	0.65	0.00	0.75	0.00	0.85	0.00	0.90	0.00	0.69
BVAR(1)-CSV	0.21	1.00**	0.24	1.00**	0.31	1.00**	0.40	1.00**	0.46	1.00**	0.54	1.00**	0.62	1.00**	0.44
DNS	1.09	0.00	1.04	0.00	1.15	0.00	1.16	0.00	1.12	0.00	1.09	0.00	1.55	0.00	1.17
TVP-QNS	0.53	0.00	0.57	0.00	0.63	0.04	0.59	0.00	0.56	0.02	0.56	0.70**	0.83	0.00	0.61
<i>12 Month-Ahead Forecast</i>															
TVP-AR(1)-SV	0.89	1.00**	0.85	1.00**	0.90	1.00**	0.92	1.00**	0.91	1.00**	0.90	1.00**	0.87	1.00**	0.89
BVAR(1)-CSV	0.83	0.93**	0.87	0.93**	0.93	0.93**	0.97	0.93**	0.99	0.94**	1.03	0.93**	1.09	0.94**	0.98
DNS	1.07	0.00	1.08	0.00	1.10	0.00	1.07	0.00	1.03	0.00	0.98	0.00	1.06	0.00	1.04
TVP-QNS	0.99	0.93**	0.99	0.93**	0.98	0.93**	0.90	0.93**	0.83	0.94**	0.76	0.93**	0.77	0.94**	0.86
<i>36 Month-Ahead Forecast</i>															
TVP-AR(1)-SV	–	0.00	–	0.00	–	0.00	–	0.00	–	0.00	–	0.00	1.37	0.00	–
BVAR(1)-CSV	1.68	0.00	1.68	0.00	1.70	0.00	1.72	0.00	1.71	0.00	1.76	0.00	1.90	0.00	1.75
DNS	1.07	0.05	1.06	0.26**	1.06	0.74**	1.03	0.05	0.99	0.00	0.96	0.00	1.03	0.00	1.02
TVP-QNS	1.06	1.00**	1.03	1.00**	1.01	1.00**	0.95	1.00**	0.90	1.00**	0.86	1.00**	0.87	1.00**	0.93

Notes: Superscripts * and ** indicate inclusion in the model confidence sets $\widehat{\mathcal{M}}_{90\%}^*$ and $\widehat{\mathcal{M}}_{75\%}^*$ respectively, as per [Hansen et al. \(2011\)](#). The reported average score is computed across all 17 maturities. A dash (‘–’) indicates that the quantile scores for the TVP-AR(1)-SV model are exceptionally large and thus omitted from the table for clarity.

4.3 In-Sample Results

Previous studies, including [Diebold and Li \(2006\)](#); [Diebold et al. \(2006, 2008\)](#); [Mumtaz and Surico \(2009\)](#); [Mönch \(2012\)](#), focused on the yield curve and its effects within a conditional mean framework. Our study is distinct from the former as it is the first to

explore the yield curve from a quantile or distributional perspective.

This section presents our empirical in-sample results. The first subsection reports posterior estimates of the yield curve factors and the decay parameter across various quantile levels. The second subsection investigates the distributional properties of short- and long-term interest rates, as well as selected Treasury maturities, during recent crises—the Great Recession and the COVID-19 pandemic. Finally, the third subsection analyses the relationship between yield curve factors and macroeconomic variables from a quantile perspective.

4.3.1 Posterior Estimates of the Decay Parameter

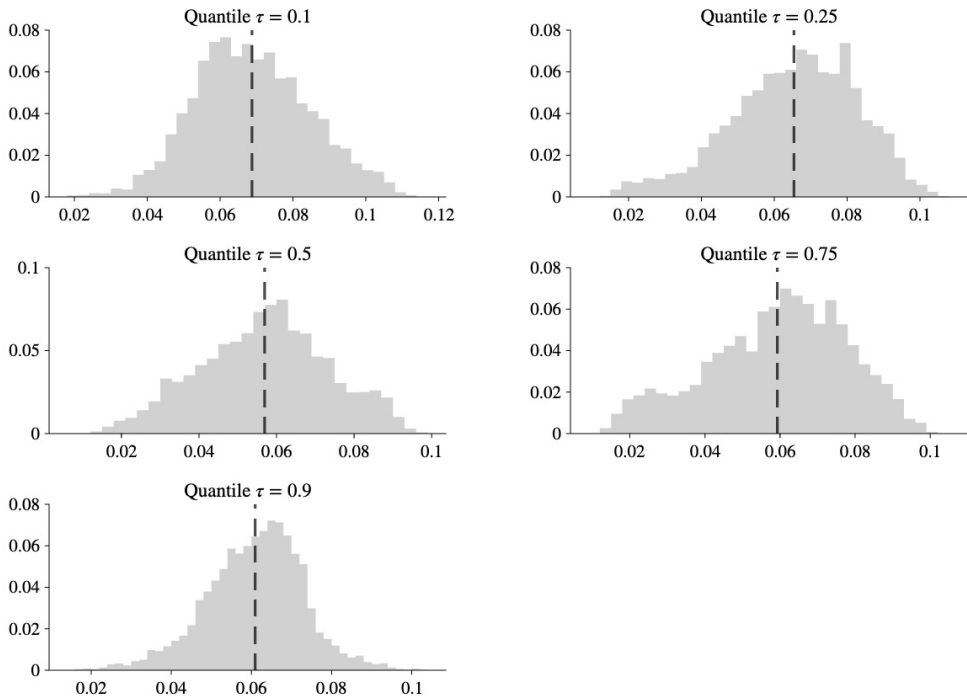


Figure 2: Posterior distribution of $\lambda(\tau)$ for the 10%, 25%, 50%, 75% and 90% quantiles, with the posterior mean (dashed line).

Figure 2 presents the posterior distribution of the decay parameter $\lambda(\tau)$ across five selected quantiles (10%, 25%, 50%, 75%, and 90%). The results indicate that, for each quantile, the posterior mass of $\lambda(\tau)$ is concentrated in the range of approximately 0.06

to 0.07. This is broadly consistent with the fixed value of $\lambda = 0.0609$ proposed by Diebold et al. (2006).

4.3.2 Quantile Yield Curve Factor Estimates

Figures 3, 4, and 5 depict the posterior mean estimates of time-varying yield curve factors at five quantile levels, providing insights into their dynamic evolution. A consistent finding across all graphs is the presence of substantial temporal variation. Beginning with the level factor, interpreted as the long-term interest rate (i.e., yield as maturity approaches infinity), a steady decline in this rate is discernible across all quantiles since the oil price crisis of the 1980s. Figure 3 reveals a distinct pattern: following both the dot-com recession in the early 2000s and the Great Recession of 2008-09, the posterior estimates for the 90th and median quantiles closely align, while those for the 10th quantile diverge. Conversely, after the COVID-19 recession, the opposite trend emerged, with the 10th and median quantiles exhibiting proximity while the 90th quantile diverged. This evidence suggests that post the early 2000s recession and the Great Recession, the distribution of the long-term interest rate skewed leftwards. In contrast, after the COVID-19 recession, the distribution skewed rightwards, likely attributed to the pronounced inflationary pressures experienced in the aftermath of the COVID-19 period.

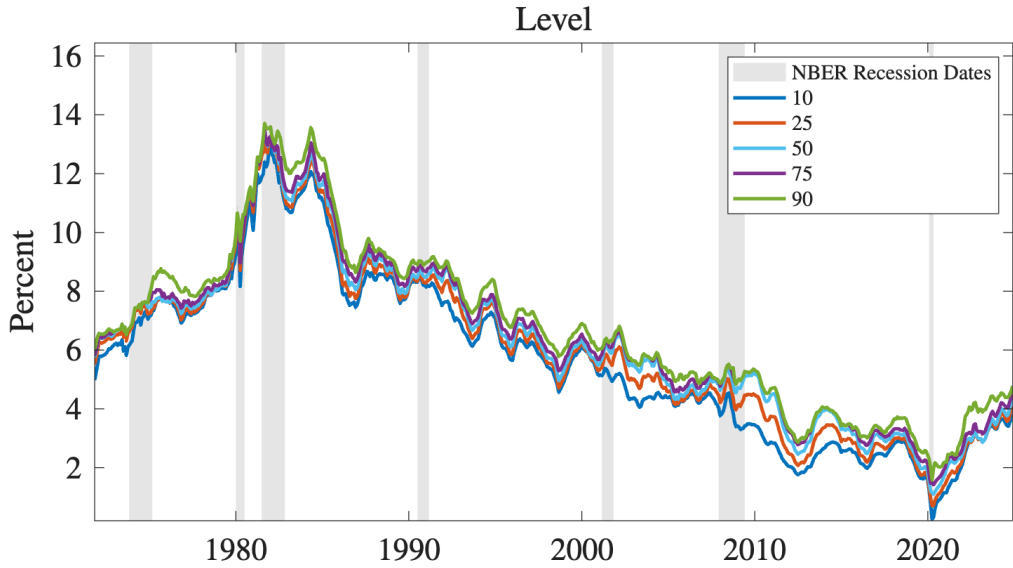


Figure 3: Posterior mean estimates of the level factor for each of the five quantiles (10%, 25%, 50%, 75%, 90%). NBER recession periods in grey shades.

Turning to the slope and curvature of the yield curve in Figures 4 and 5, the degree of uncertainty associated with these factors varies over time. Notably, the curvature factor exhibits higher volatility across all quantiles than its slope counterpart.¹ A distinct pattern is evident before 1985, where the posterior estimates for the slope factor across all five quantiles are closely clustered, indicating a period of low uncertainty. In contrast, during the oil price crisis of the 1980s, the curvature factor displayed substantial dispersion across quantiles.

¹We impose the monotonicity constraint specified in equation (18) on the short-term interest rate, defined as the sum of the level and slope factors. Figure 10 in the appendix displays the posterior estimates of the short-term rate across the five quantiles, which exhibit no crossing and are thus consistent with the imposed constraint. However, this restriction does not imply monotonicity in the slope factor alone, which may still exhibit crossings across quantiles. In contrast, crossings in the conditional quantiles of the curvature factor are not of concern, as the curvature does not correspond directly to any specific yield maturity.

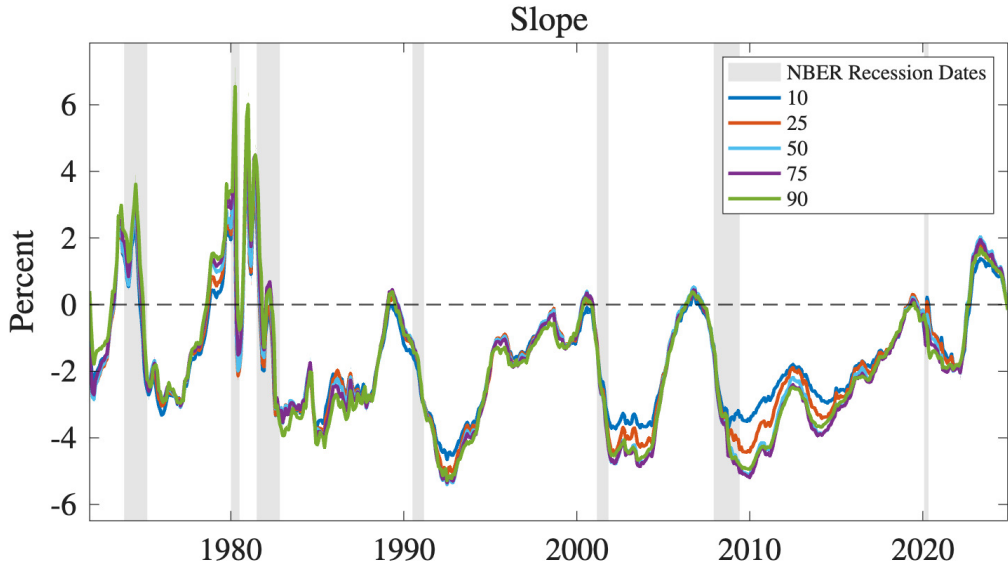


Figure 4: Posterior mean estimates of the slope factor for each of the five quantiles (10%, 25%, 50%, 75%, 90%). NBER recession periods in grey shades.

Post-recessionary periods following the early 1990s, the 2000s, and the Great Recession of 2008-09 reveal elevated uncertainty in both slope and curvature factors. Specifically, convergence is observed between the median and the 90th quantile, with the 10th quantile exhibiting a discernible deviation from this convergent trajectory. In the aftermath of the COVID-19 recession, a reverse trajectory emerges, with the 90th quantile diverging from the 10th and median quantiles. The associated uncertainty surrounding both factors appears comparatively subdued compared to the preceding recessions of the 2000s. Both the early 2000s recession and the Great Recession were attributed to financial crises. Our empirical findings suggest a potential connection between periods following financial crises and increased uncertainty in the slope and curvature of the yield curve.

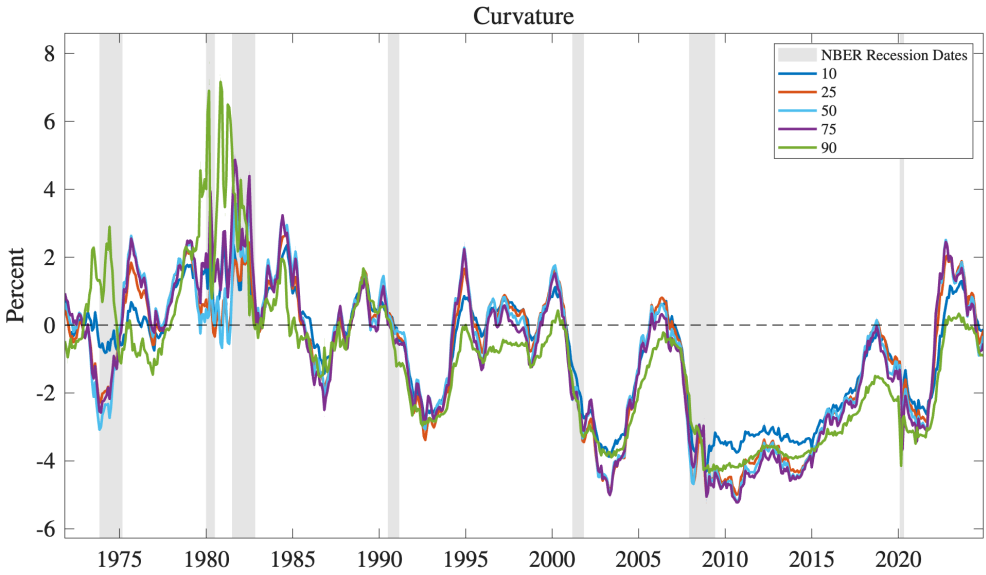


Figure 5: Posterior mean estimates of the curvature factor for each of the five quantiles (10%, 25%, 50%, 75%, 90%). NBER recession periods in grey shades.

It is worthwhile mentioning that these results could not be obtained using a conditional mean approach, which is instead able to produce estimates of the mean yield factors over time. Conversely, the proposed quantile approach enables deeper and more detailed analyses of the term structure while maintaining a low computational cost.

4.3.3 Distributional Characteristics of Treasury Yields Across the Term Structure

The proposed novel framework offers a distinct advantage by enabling the examination of the distributional properties of both short- and long-term interest rates, as well as selected yield maturities, over time. As previously discussed, the long-term interest rate is identified with the level factor, whereas the short-term interest rate reflects a combination of the level and slope factors. We follow the methodology outlined by [Mitchell et al. \(2024\)](#) to construct the empirical distributions of these rates and maturities. Specifically, we adopt an equal-weighting scheme to aggregate all MCMC draws across five quantiles and apply the Epanechnikov kernel, as proposed by [Gaglianone and Lima \(2012\)](#).

The previous analysis revealed an increase in the degree of dispersion among quantiles during post-recessionary periods, particularly in the 2000s. Expanding on this finding, we investigate whether the distributional features of short- and long-term interest rates exhibit temporal variations across the two most recent recessions. Figure 6 illustrates the distributions of both short- and long-term interest rates for selected months preceding and following the Great Recession and the COVID-19 recession.

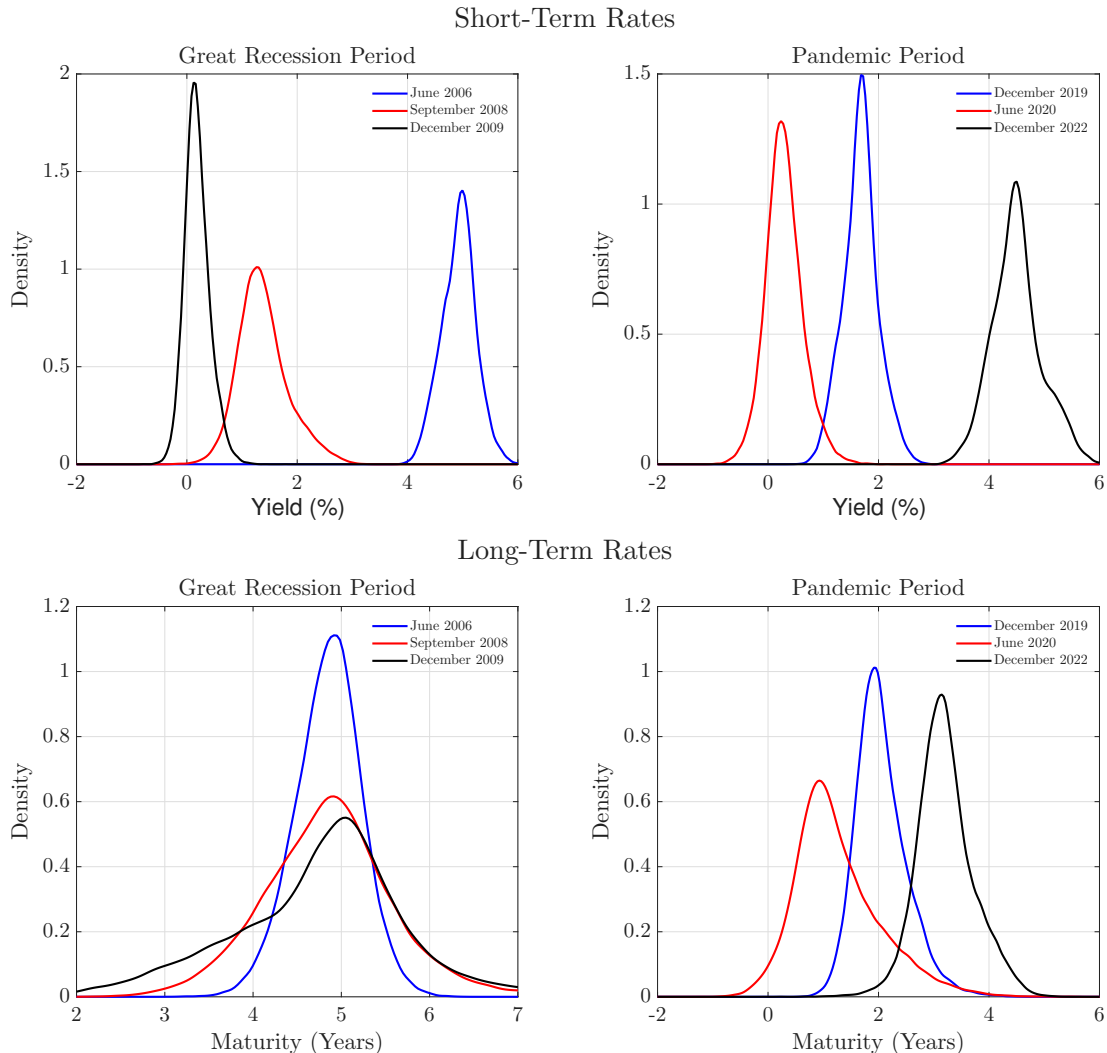


Figure 6: Distribution of the short-term and long-term (level) factors during the Great Recession (left) and the COVID-19 pandemic (right).

Focusing first on the short-term interest rate, we observe clear evidence of a pronounced distributional shift across the three selected months during both the Great Recession and the COVID-19 recession. In particular, following the COVID-19 reces-

sion (December 2020), the distribution of the short-term rate becomes less symmetric and exhibits increased negative skewness.

Turning to the long-term interest rate, distributional changes appear more pronounced during the COVID-19 recession than during the Great Recession. After the Great Recession (December 2009), the distribution becomes more negatively skewed. In contrast, during the COVID-19 recession, the distribution shifts towards positive skewness, indicating a different form of market adjustment at the long end of the yield curve.

Figure 7 presents the estimated conditional distributions of three selected Treasury maturities—3 months, 3 years, and 10 years—representing the short, intermediate, and long segments of the yield curve, respectively, across the two crisis periods. Prior to the Great Recession, the distributions of these maturities are relatively similar. However, in the aftermath of the Great Recession, we observe a clear location shift across all maturities, with the 10-year maturity displaying increased left-skewness. During the COVID-19 recession, only the long end of the yield curve undergoes a location shift, accompanied by greater dispersion. Following the COVID-19 episode, all three maturities exhibit a location shift, with the short and intermediate maturities also displaying increased negative skewness.

These results indicate that short- and long-term interest rates, as well as selected yield maturities, experience heightened skewness and asymmetry during recessionary periods. This highlights the empirical relevance of quantile-based approaches, which allow for a more flexible representation of the conditional distribution—particularly in the tails—than traditional factor models such as Nelson-Siegel, which impose symmetry and are limited in their ability to capture such nonlinearities.

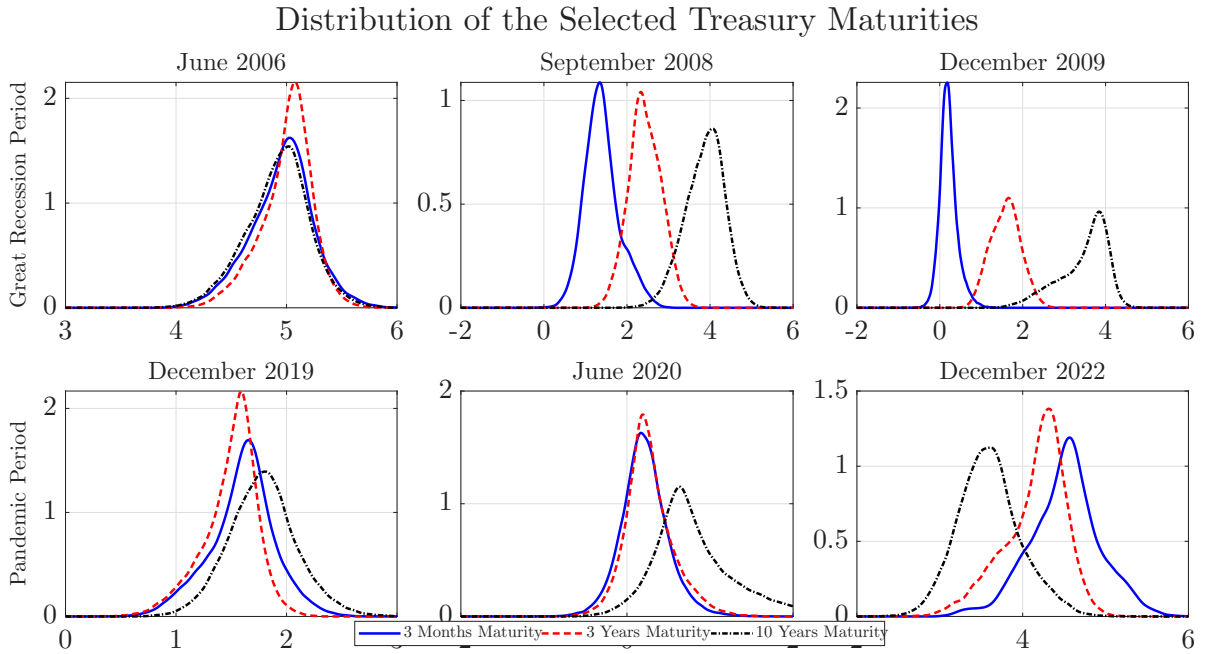


Figure 7: Distribution of the 3-month, 3-year, and 10-year Treasury yields during the Great Recession (top panel) and the COVID-19 pandemic period (bottom panel). The solid blue line corresponds to the 3-month maturity, the red dashed line represents the 3-year maturity, and the black dashed line denotes the 10-year maturity.

4.3.4 The Interaction between the Yield Curve and Macroeconomy

The proposed framework, as specified in Equation (9), enables an in-depth analysis of the dynamic interaction between yield curve factors and macroeconomic variables by incorporating a VAR-like state equation. To explore these interactions, we compute the generalized forecast error variance decomposition (GFEVD) across five quantiles, evaluating the contribution of shocks to yield curve factors on macroeconomic variables—and vice versa—as illustrated in Figures 8 and 9, respectively.

We begin by examining the effects of yield curve shocks on macroeconomic variables (Figure 8). The analysis reveals that curvature shocks generate heterogeneous impacts across the distribution of macroeconomic outcomes. Notably, these shocks have a more pronounced effect on the upper tail of all three macroeconomic variables—particularly at longer forecast horizons—indicating heightened sensitivity in more expansionary states of the economy. In contrast, level shocks increasingly influence the lower tail of industrial production over time, suggesting growing downside risks in response to shifts in the

overall level of the yield curve.

We next assess the influence of macroeconomic shocks on the yield curve (Figure 9). Shocks to industrial production significantly affect the lower tails of all three yield curve factors, implying that negative real activity shocks disproportionately compress the yield distribution. By contrast, inflation shocks primarily impact the upper tails of the slope and curvature factors, with these effects intensifying at longer horizons—consistent with rising term premia during inflationary episodes. Additionally, federal funds rate shocks increasingly affect the upper tail of the level factor over time, underscoring the asymmetric transmission of monetary policy to the term structure.

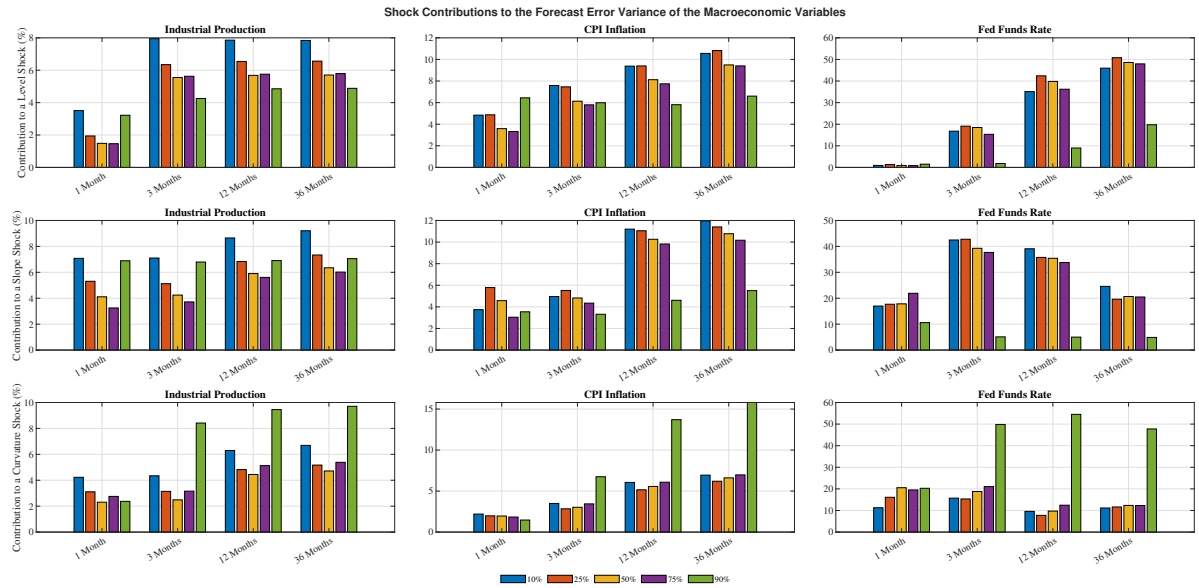


Figure 8: Posterior estimates of the generalized forecast error variance decomposition for the macroeconomic variables (columns) on Yield Curve Factors (rows). The colored bars represent different quantiles: blue (10%), orange (25%), yellow (50%), purple (75%), and green (90%).

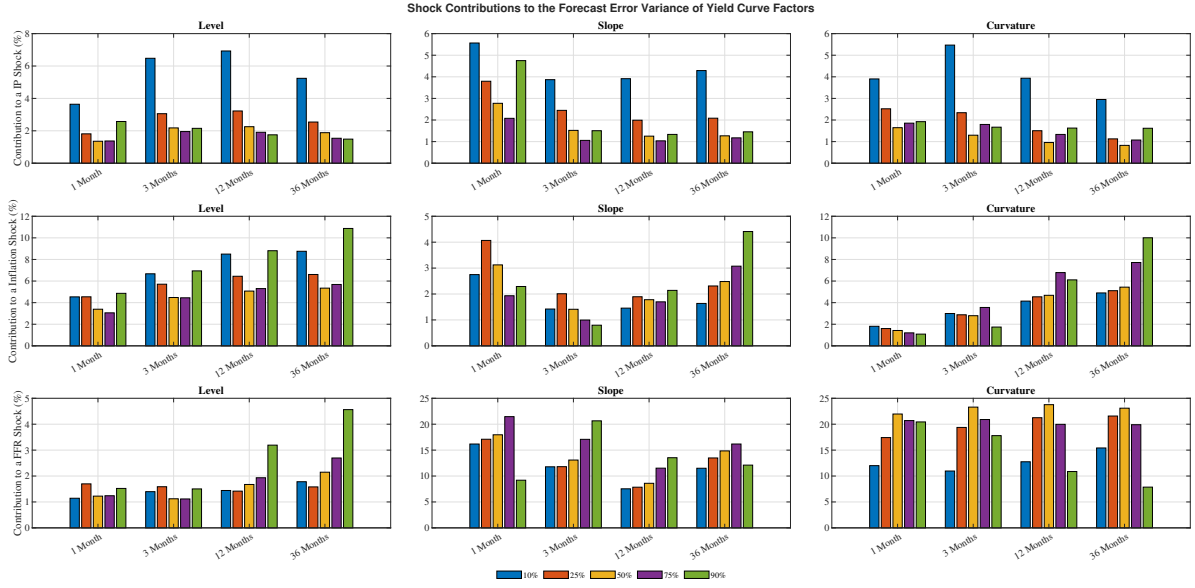


Figure 9: Posterior estimates of the generalized forecast error variance decomposition for the Yield Curve Factors (columns) on Yield Curve Factors (rows). The colored bars represent different quantiles: blue (10%), orange (25%), yellow (50%), purple (75%), and green (90%).

In summary, these results provide robust evidence that the interaction between yield curve factors and macroeconomic variables is highly dependent on the quantile considered. This highlights the importance of employing quantile-based approaches, which can capture distributional asymmetries and tail behavior that standard linear models may overlook.

5 Conclusions

This study introduces a novel time-varying parameter quantile Nelson-Siegel (TVP-QR-NS) model, estimated within a Bayesian framework, to analyse the US term structure of interest rates. The out-of-sample forecasting results demonstrate that the TVP-QR-NS model consistently outperforms conventional benchmarks in forecasting tail risks, particularly at longer horizons and for long-term maturities. Importantly, it is the only model consistently included in the model confidence sets for these maturities and horizons, while standard conditional mean models are frequently excluded. The in-sample analysis reveals significant dispersion in yield curve factors across quantiles,

especially following recessionary periods. The analysis also uncovers pronounced shifts in the distributions of short- and long-term interest rates—as well as yields at selected maturities—during the Great Recession and the COVID-19 pandemic, highlighting the importance of capturing variation across both time and quantiles. In addition, strong evidence is found of quantile-dependent dynamics in the relationship between yield curve factors and macroeconomic conditions. Overall, these findings highlight the robustness and practical relevance of the TVP-QR-NS framework for risk management and macro-financial policy analysis.

References

Benzoni, L., O. Chyruk, and D. Kelley (2018). Why does the yield-curve slope predict recessions? Technical Report 404, Chicago FED Letter.

Bianchi, F., H. Mumtaz, and P. Surico (2009). The great moderation of the term structure of UK interest rates. *Journal of Monetary Economics* 56(6), 856–871.

Carriero, A., T. E. Clark, and M. Marcellino (2022). Nowcasting tail risk to economic activity at a weekly frequency. *Journal of Applied Econometrics* 37(5), 843–866.

Chan, J. C. (2020). Large Bayesian vector autoregressions. In P. Fuleky (Ed.), *Macroeconomic Forecasting in the Era of Big Data*. Springer.

Chan, J. C., E. Eisenstat, and R. W. Strachan (2020). Reducing the state space dimension in a large TVP-VAR. *Journal of Econometrics* 218(1), 105–118.

Chan, J. C. and I. Jeliazkov (2009). Efficient simulation and integrated likelihood estimation in state space models. *International Journal of Mathematical Modelling and Numerical Optimisation* 1(1-2), 101–120.

Chernozhukov, V., I. Fernández-Val, and A. Galichon (2010). Quantile and probability curves without crossing. *Econometrica* 78(3), 1093–1125.

Clark, T. E., F. Huber, G. Koop, M. Marcellino, and M. Pfarrhofer (2024). Investigating growth-at-risk using a multicountry nonparametric quantile factor model. *Journal of Business & Economic Statistics* 42(4), 1302–1317.

Coroneo, L., D. Giannone, and M. Modugno (2016). Unspanned macroeconomic factors in the yield curve. *Journal of Business & Economic Statistics* 34(3), 472–485.

Diebold, F. X. and C. Li (2006). Forecasting the term structure of government bond yields. *Journal of Econometrics* 130(2), 337–364.

Diebold, F. X., C. Li, and V. Z. Yue (2008). Global yield curve dynamics and interactions: a dynamic Nelson–Siegel approach. *Journal of Econometrics* 146(2), 351–363.

Diebold, F. X., G. D. Rudebusch, and S. B. Aruoba (2006). The macroeconomy and the yield curve: a dynamic latent factor approach. *Journal of Econometrics* 131(1-2), 309–338.

Fernandes, M. and F. Vieira (2019). A dynamic Nelson–Siegel model with forward-looking macroeconomic factors for the yield curve in the US. *Journal of Economic Dynamics and Control* 106, 103720.

Fonseca, L., P. McQuade, I. Van Robays, and A. L. Vladu (2023). The inversion of the yield curve and its information content in the euro area and the United States. ECB Economic Bulletin Issue 7.

Gaglianone, W. P. and L. R. Lima (2012). Constructing density forecasts from quantile regressions. *Journal of Money, Credit and Banking* 44(8), 1589–1607.

Giacomini, R. and I. Komunjer (2005). Evaluation and combination of conditional quantile forecasts. *Journal of Business & Economic Statistics* 23(4), 416–431.

Gneiting, T. and R. Ranjan (2011). Comparing density forecasts using threshold-and quantile-weighted scoring rules. *Journal of Business & Economic Statistics* 29(3), 411–422.

Gürkaynak, R. S., B. Sack, and J. H. Wright (2007). The US Treasury yield curve: 1961 to the present. *Journal of Monetary Economics* 54(8), 2291–2304.

Han, Y., A. Jiao, and J. Ma (2021). The predictive power of Nelson–Siegel factor loadings for the real economy. *Journal of Empirical Finance* 64, 95–127.

Hansen, P. R., A. Lunde, and J. M. Nason (2011). The model confidence set. *Econometrica* 79(2), 453–497.

Haubrich, J. G. (2021, 2024/01/09). Does the yield curve predict output? *Annual Review of Financial Economics* 13(1), 341–362.

Koenker, R. and G. Bassett (1978). Regression quantiles. *Econometrica*, 33–50.

Koopman, S. J. and M. van der Wel (2013). Forecasting the US term structure of interest rates using a macroeconomic smooth dynamic factor model. *International Journal of Forecasting* 29(4), 676–694.

Korobilis, D. and M. Schröder (2024). Probabilistic Quantile Factor Analysis. *Journal of Business & Economic Statistics* (3), 530 — 543.

Korobilis, D. and M. Schröder (2025). Monitoring multi-country macroeconomic risk: A quantile factor-augmented vector autoregressive (QFAVAR) approach. *Journal of Econometrics*, 105730.

Kotz, S., T. Kozubowski, and K. Podgórski (2001). *The Laplace distribution and generalizations: a revisit with applications to communications, economics, engineering, and finance*. Number 183. Springer Science & Business Media.

Lenza, M., I. Moutachaker, and J. Paredes (2025). Density forecasts of inflation: A quantile regression forest approach. *European Economic Review*, 105079.

Liu, Y. and J. C. Wu (2021). Reconstructing the yield curve. *Journal of Financial Economics* 142(3), 1395–1425.

Mitchell, J., A. Poon, and D. Zhu (2024). Constructing density forecasts from quantile regressions: Multimodality in macrofinancial dynamics. *Journal of Applied Econometrics* 39(5), 790–812.

Mönch, E. (2012). Term structure surprises: the predictive content of curvature, level, and slope. *Journal of Applied Econometrics* 27(4), 574–602.

Mumtaz, H. and P. Surico (2009). Time-varying yield curve dynamics and monetary policy. *Journal of Applied Econometrics* 24(6), 895–913.

Nelson, C. R. and A. F. Siegel (1987). Parsimonious Modeling of Yield Curves. *The Journal of Business* 60(4), 473–489.

Petrella, L. and V. Raponi (2019). Joint estimation of conditional quantiles in multivariate linear regression models with an application to financial distress. *Journal of Multivariate Analysis* 173, 70–84.

Ritter, C. and M. A. Tanner (1992). Facilitating the Gibbs Sampler: The Gibbs Stopper and the Griddy-Gibbs Sampler. *Journal of the American Statistical Association* 87(419), 861–868.

Yu, K. and R. A. Moyeed (2001). Bayesian quantile regression. *Statistics & Probability Letters* 54(4), 437–447.

A Appendix

A.1 Sampling the Decay Parameter

As mentioned above, it has so far been common practice to fix λ to be a particular value. On the other hand, we are agnostic and estimate $\lambda(\tau)$ given the data for each quantile. Given a uniform prior for $\lambda(\tau)$, $p(\lambda(\tau)) \sim U(a, b)$, the conditional posterior of $(\lambda(\tau)|\bullet)$ is given by

$$(\lambda(\tau)|\bullet) \propto p(\mathbf{Y}, \mathbf{w}|\boldsymbol{\beta})p(\lambda(\tau)),$$

where $a < \lambda(\tau) < b$. Since the support of this conditional density is bounded and non-standard, we draw from this conditional density using a Griddy-Gibbs step (Ritter and Tanner, 1992). This is done using the following steps:

1. Construct a grid with grid points $\hat{\lambda}(\tau)_1, \dots, \hat{\lambda}(\tau)_R$, where $\hat{\lambda}(\tau)_1 = a$ and $\hat{\lambda}(\tau)_R = b$.
2. Compute $F_i = \sum_{j=1}^i p(\hat{\lambda}(\tau)_j|\bullet)$.
3. Generate U from a standard uniform distribution.
4. Find the smallest positive integer k such that $F_k \geq U$ and return $\lambda(\tau) = \hat{\lambda}(\tau)_k$.

A.2 Additional In-Sample Results

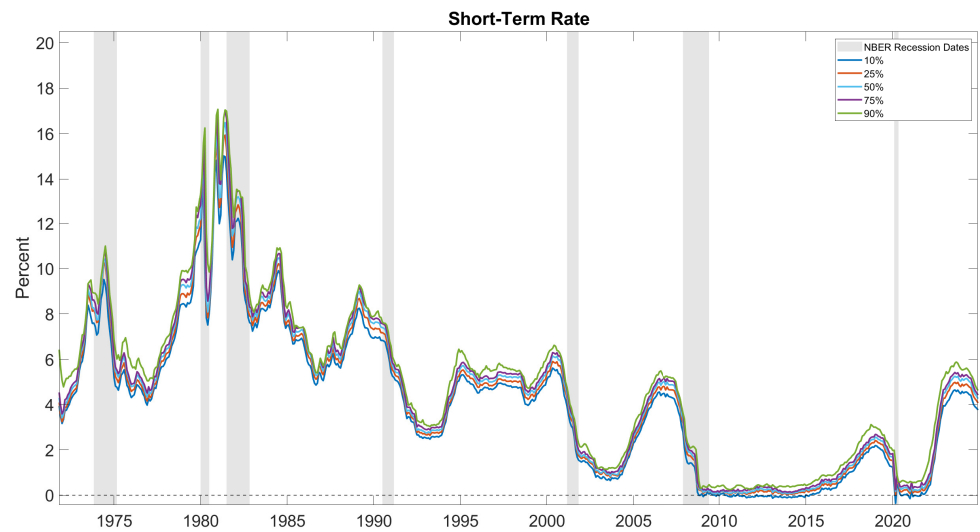


Figure 10: Posterior mean estimates of the short-term rate (Level + Slope) for each of the five quantiles (10%, 25%, 50%, 75%, 90%). NBER recession periods in grey shades.